RESEARCH ARTICLE

DCT-SVD Based Hybrid Approach for Digital Watermarking of Medical Images

Emine Aksu[1] and **Murat Karakoyun**[2,*]

[1] Industrial Engineering, Institute of Science and Technology, Necmettin Erbakan University, Konya 42090, Turkey
[2] Computer Engineering, Faculty of Engineering, Necmettin Erbakan University, Konya 42090, Turkey

Abstract

This study addresses invisible watermarking techniques aimed at preserving patient privacy during the sharing of medical images. Digital watermarking is a significant method for protecting the confidentiality of patient data by securely embedding personal information into medical images. In this study, three different strategies were developed and compared using a DCT-SVD-based hybrid invisible watermarking technique. In the first method, the host image and the watermark were of the same size, and direct embedding was applied. In the second method, the host image was divided into sixteen 128x128 blocks, and the watermark was segmented accordingly and embedded into each block individually. In the third and proposed method, non-diagnostic regions of the image—referred to as dead zones—were automatically detected, and the watermark was embedded only into these areas. This approach preserved the relevant medical data while minimizing image distortion. When the scaling factor was set to 0.01, PSNR values exceeded 40 for most images, and SSIM values were above 0.9. The results demonstrated that the proposed method outperformed the other two in terms of both imperceptibility and robustness.

Keywords: digital watermarking, DCT, SVD, medical images, patient privacy, image processing.

1 Introduction

Digital communication tools, including images, sound, film, and multimedia, have advanced significantly, raising copyright issues that image encryption alone cannot fully resolve. One solution is embedding information within images, a practice known as image watermarking, which helps copyright holders prove ownership without altering the image's appearance. This can be either visible or invisible, with invisible watermarking being more commonly preferred for privacy and security reasons [2]. This study focuses on invisible watermarking.

Watermarking has gained attention in areas like copyright protection, data authenticity, and information embedding. Various methods have been proposed, some focusing on invisibility, others on robustness, or a combination of both [3]. In healthcare, watermarking is crucial for protecting medical images, which are shared across institutions for diagnostic purposes. The challenge is to preserve image quality while maintaining robust watermarking, particularly in regions unrelated to diagnostic content,

Submitted: 30 September 2025
Accepted: 27 November 2025
Published: 31 January 2026

Vol. 2, **No.** 1, 2026.
10.62762/TSEL.2025.219908

***Corresponding author:**
Murat Karakoyun
mkarakoyun@erbakan.edu.tr

Citation
Aksu, E., & Karakoyun, M. (2026). DCT-SVD Based Hybrid Approach for Digital Watermarking of Medical Images. *ICCK Transactions on Swarm and Evolutionary Learning*, 2(1), 1–18.

to prevent interference [4]. These issues highlight the need for further advancements in maintaining the authenticity and integrity of medical images [5].

The aim of this study is to embed a hidden message, which includes the patient's radiology report, into specific regions of a medical image. After applying the Discrete Cosine Transform (DCT) to the host image, watermarking is performed by combining the singular values of the host image and watermark image. The goal is to minimize the distortion in the host image while ensuring the robust extraction of the watermark. A literature review of similar research was conducted, considering the characteristics and qualities of medical images. Other digital watermarking algorithms were evaluated to develop a more reliable digital watermarking algorithm for medical images. In this study, a DCT based invisible watermarking technique using Singular Value Decomposition (SVD) was applied, and the ability of the new images to preserve the hidden information was investigated. Then, watermark extraction was performed, and the success of the methods was tested. During the application, 13 medical images were used as hosts, and 2 radiological reports were used as watermarks. The similarity between the original and watermarked images was measured using metrics such as Peak-Signal-to-Noise Ratio (PSNR), Mean Squared Error (MSE), Normalized Correlation (NC), and Structural Similarity Index (SSIM).

2 Related Work

The practice of embedding hidden messages has evolved from Steganography to Cryptology and Digital Watermarking, with numerous studies conducted in this field. In 2004, Alghoniemy et al. [6] developed a watermarking technique that employs geometric shapes in the frequency domain. The robustness of this method was evaluated by introducing white noise at varying levels of intensity to the watermarked image, demonstrating its significant resistance to noise disturbances. In a study by Solachidis and Pitas [1], a circular convolving image watermarking method was introduced. In this method, a circular convolving watermark is added in the frequency domain. The multiplicative addition method was used to keep the watermark visibility ratio low, and correlation was used to test the presence of the watermark in the image. Experimental results showed that the method was resistant to disruptive effects such as JPEG compression, filtering, noise addition, cropping, rotation, and scaling. An algorithm using the Discrete Wavelet Transform (DWT) method was developed to make the watermarked element resistant to attacks by Elbaşı. In DWT, both the LL and HH bands were used to add PRN, making the watermark resistant to attacks. It was concluded that using both bands in the DWT method resulted in more successful watermarking [3].

In 2009, Aslantas [7] developed an SVD-based image watermarking method, examining the effectiveness of DCT, DFT, and DWT techniques. Various attacks were applied to the watermarked images, and it was observed that the DFT-SVD-based method performed better when the optimal scaling factor was selected. In another study by Aslantaş et al. [8], a DWT-SVD-based image watermarking method was investigated. The watermark scaling factors were optimally determined using the Particle Swarm Optimization (PSO) algorithm, and the proposed technique outperformed methods that used fixed scaling factors.

In the study by Aslantaş and Öz [9], a watermarking technique based on SVD and Differential Evolution Algorithm (DEA) was developed. The watermarked image was obtained by adding the scaled watermark with multiple scaling factors to the singular values of the image. An objective function was defined to evaluate both robustness and visibility, and it was optimized using DEA. As a result, the lowest level of distortion in the image and the highest resistance to attacks were achieved. Furat and Oral [10] examined data storage methods and digital image watermarking algorithms in past studies. These watermarking algorithms were explained in detail, and it was emphasized that these algorithms are generally success-oriented toward specific goals. In the study by Dogan et al. [11], a watermarking application for color images was implemented using the SVD method. In their study, an iris image was embedded in a facial image using the SVD method. During the watermarking process, the watermark was embedded in its original form, regardless of the scaling value used in the SVD-based methods. The results showed that the PSNR values of the images exposed to attacks were higher and more successful compared to similar studies. In the study by Ustubioglu and Ulutas [12], Region of Interest (ROI) and Region of Non-Interest (RONI) areas were used to securely store patient information and maintain the integrity of medical images. Literature studies required small ROI, while the proposed method allowed ROI to be up to 65%. Experimental results showed that the method was effective with high PSNR and Normalized Correlation (NC) values. In the study by Mamuti and Kazan [5], color images were separated into color channels, and each channel was processed with different watermarking algorithms. The performance of the proposed digital watermarking algorithm was evaluated and analyzed using NC and PSNR. Experimental results showed that the algorithm was successful and effective in achieving acceptable image quality. In the study by Karakış and Gürkahraman [4], personal patient information and radiology reports in medical images' file headers were encrypted using the AES-256 algorithm. These encrypted data were hidden in pixels in irrelevant areas of the host images, identified using histogram statistics. The watermarking process was performed by combining the singular values obtained from the message and the host image using DWT and SVD methods, and the method was evaluated. The study found that the developed method was imperceptible, resistant to attacks, and had high data hiding capacity compared to similar works in the literature. In the study by Mohammed et al. [2], a hybrid method was used for embedding patient's private information into images by performing DCT and SVD-based image watermarking. PSNR and NC were used for performance evaluation. The results showed that the proposed method was secure and robust. In the study by Priyanka and Maheshkar [13], a new fragile watermarking method based on DCT and trigonometric functions for image authentication was proposed. Grayscale images were divided into 4×4 overlapping blocks, and DCT was applied to each block, with the DC component selected. The selected value was converted into control bits and embedded into the least significant bits of the block as the watermark. Experimental results showed that the method preserved the quality of the watermarked image, made the watermark undetectable, and was successful in detecting regional attacks. In the study by Yıldız et al., watermarking methods used to protect copyright violations and personal data privacy in digital images were examined. A hybrid watermarking technique combining DWT, DCT and SVD was developed, and various types of noise were added to the watermarked images. Optimization algorithms such as Bacterial Foraging Optimization (BFO) and PSO were used to improve the watermark extraction process, which was evaluated using performance metrics like PSNR, Normalized Cross-Correlation (NCC), and Interference Factor (IF). The results showed that the applied techniques were effective, yielding successful outcomes in both watermarking and watermark extraction processes [14].

3 Methodology

In this study, non-blind invisible watermarking was applied, and reports were embedded into medical images using three different DCT-SVD-based methods, with the watermark being extracted afterward. PSNR, MSE, NC, and SSIM values were compared for different images and reports.

3.1 Images Used

In the experiment phase, a total of 13 medical images were used as host images. These were selected from different imaging modalities: 10 vertebra (MRI), 2 abdomen (ultrasound), and 1 skull radiograph (CR). All images were in DICOM format, grayscale, and had a size of 512x512 pixels. Additionally, two radiology reports were used as watermarks and labeled as W1 and W2. The host images were numbered from I1 to I13. This structure allowed the proposed method to be tested across different anatomical regions and imaging modalities.

3.2 DCT-SVD Based Hybrid Watermarking Methods

In this study, three different methods were compared using a DCT-SVD-based hybrid watermarking technique. In the first method, direct watermarking was applied to a host image that was the same size as the watermark. In the second method, the host image was divided into 16 blocks (4x4), and the watermark was embedded into each block. In the third method, the watermark was embedded only into the non-relevant (non-diagnostic) regions of the host image. The same watermarking technique was used in all methods, with the differences arising from the embedding location and image dimensions.

3.2.1 Method 1: Equal-Sized Host Image and Watermark

Method 1 was implemented by directly embedding the watermark into the entire host image. Both images are grayscale and have a size of 512×512 pixels. The images were preprocessed using rgb2gray and im2double functions to make them ready for processing. A representative illustration of the host image and the watermark is shown in Figure 1.

The watermarking process begins by applying the DCT to the host image, followed by the application of SVD to the DCT coefficients to obtain the singular values. The same process is applied to the watermark image, and the resulting singular values are added to those

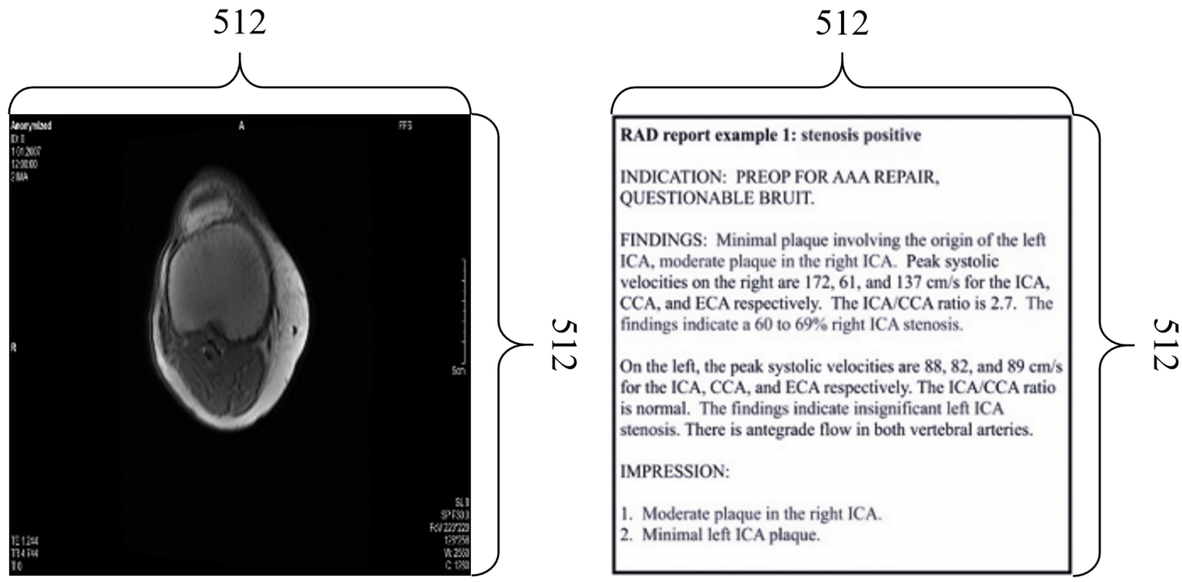

Figure 1. Representative illustration of the host image and the watermark for Method 1.

of the host image using an appropriate scaling factor. The watermarked image is then reconstructed using inverse SVD and inverse DCT.

In the extraction phase, DCT and SVD are applied to the watermarked image, and the singular values of the watermark are retrieved by computing the difference between the singular values of the host and watermarked images. The watermark is then reconstructed accordingly.

3.2.2 *Method 2: Block-Based Host Image and Watermark*

Method 2 is based on dividing the host image into 16 sub-blocks arranged in a 4×4 grid, each measuring 128×128 pixels. The resized watermark image is embedded separately into each block using the DCT-SVD-based hybrid watermarking method. This approach ensures that the watermark information is evenly distributed across the image, resulting in a more balanced watermarking structure while preserving visual integrity. Additionally, the block-based processing enhances resistance against localized attacks and facilitates the extraction of the watermark. A representative illustration of the host image and the watermark is shown in Figure 2.

During the watermarking process, after obtaining the DCT coefficients of each block, SVD is applied to these coefficients. The singular values of the watermark image are embedded into these SVD components using a predefined scaling factor. The watermark extraction process is performed in a similar manner: DCT followed by SVD is applied to the target block, allowing the watermark information to be successfully retrieved.

3.2.3 *Method 3 (Proposed Approach): Embedding the Segmented Watermark into Non-Informative Regions*

Method 3 begins by selecting both the host and watermark images in grayscale format with dimensions of 512×512 pixels. The main objective of this method is to minimize distortion that may occur in medical images during the watermarking process. Based on the previously successful DCT-SVD-based hybrid watermarking approach, this method simultaneously addresses image quality and patient data security.

The novelty of this method lies in its ability to automatically detect "non-informative" or "dead zones" frequently observed in medical images—areas that contain no diagnostic information—and embed the watermark only into these regions. This ensures that diagnostically critical parts of the image remain entirely intact. Thus, patient reports can be securely embedded without damaging meaningful information in the image.

The method is primarily based on arithmetic matrix operations and analyzes transitions between black (non-informative) and white (informative) regions in the grayscale plane. These black regions, often used for patient details such as name or date, are effectively utilized for report watermarking through the proposed algorithm. As a result, patient privacy is preserved, and diagnostic quality is maintained. The steps of the proposed method can be summarized as follows:

- Step 1: The process starts with the preparation

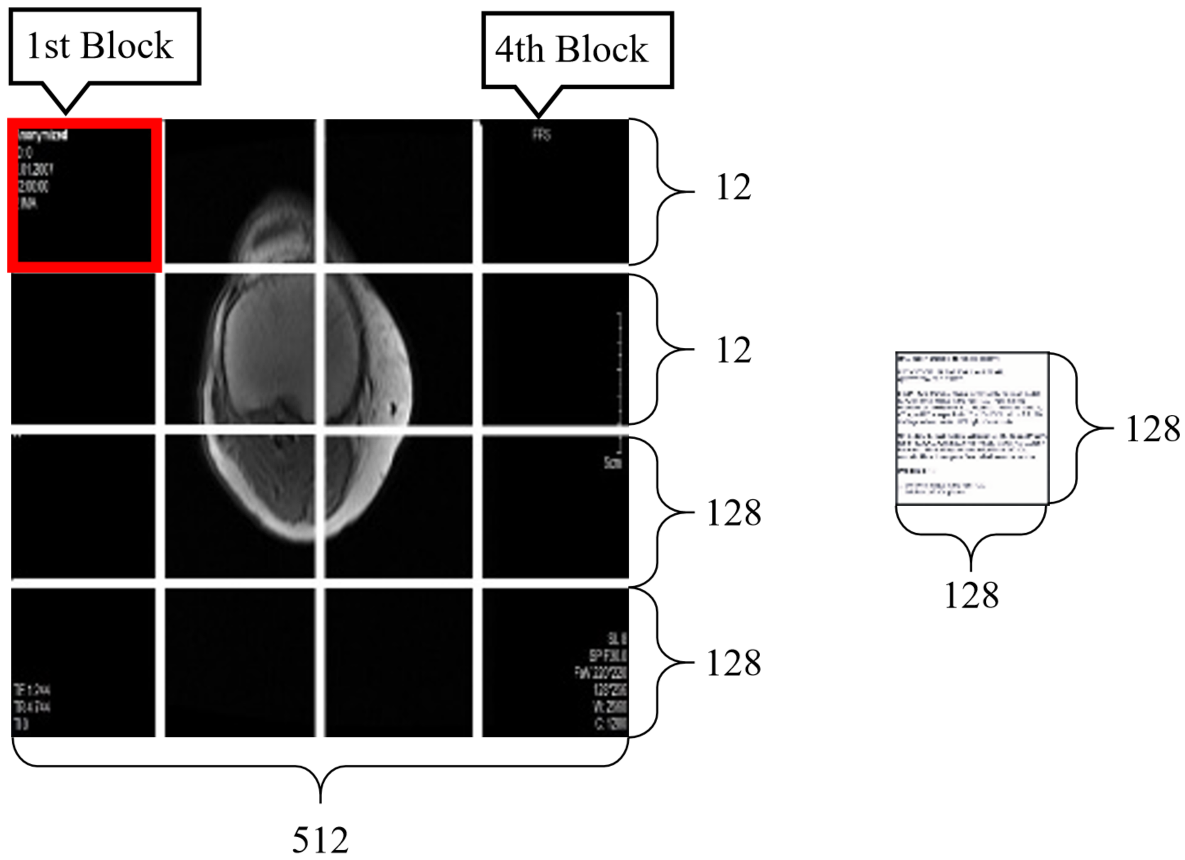

Figure 2. Representative illustration of the host image and the watermark for Method 2.

of the medical image and the watermark report. RGB images are converted to grayscale using the rgb2gray function to make them suitable for processing.

- Step 2: A matrix called matrix_list, which contains the column-wise pixel sums of the medical image, is generated. This matrix represents the total pixel value for each column.
- Step 3: Threshold values (val_high and val_low) are determined on a column basis. These values are used to distinguish between informative and non-informative regions and guide where the watermark should be placed.
- Step 4: The patient report image is resized to fit the identified non-informative regions. The imresize function is used to align the watermark image with the carrier image dimensions.
- Step 5: The resized report image is prepared so that its central part remains black and is aligned with the medical image. This ensures that informative regions are preserved and the watermark is embedded only into dead zones. At this stage, the image is ready for the watermark embedding and extraction process, just like in Method 1. In this way, patient data is securely embedded, and diagnostic integrity is preserved.
- Step 6: A two-dimensional DCT is applied to the medical image using the dct2 function. The resulting DCT coefficients are then processed using SVD to decompose the image into its components.
- Step 7: The new watermark, which has been segmented and resized, is also processed using SVD. This yields the singular values and orthogonal matrices of both images.
- Step 8: The singular values of the watermark are multiplied by an appropriate scaling factor (e.g., 0.01) and added to the singular values of the DCT coefficients of the host image. This allows for invisible watermark integration while maintaining recoverability.
- Step 9: Finally, inverse SVD and inverse DCT operations are performed to obtain the watermarked image. These steps reconstruct the original host image and watermark components. The inverse processes regenerate the image data, resulting in the final watermarked image.

A representative illustration of the host image and the segmented watermark used in the proposed approach (Method 3) is presented in detail in Figure 3. The block diagram of embedding the segmented watermark into the host image using the DCT-SVD-based hybrid watermarking technique is shown in Figure 4. The diagram of the operations performed during the watermark extraction process for Method 3 is shown in Figure 5.

In this study, human intervention was reduced through the automatic detection of dead zones, and the method demonstrated broad applicability and high performance in tests conducted on different types of medical images. The performance was validated using the PSNR, SSIM, MSE, and NC metrics.

Optimization of the Scaling Factor: The scaling factor (SF) is a critical parameter governing the fundamental trade-off between the imperceptibility of the watermarked host image and the robustness of the extracted watermark. To automate and optimize this crucial parameter selection, we can formulate the SF determination as a single-objective optimization problem and employ the Differential Evolution (DE) algorithm to solve it. DE is a population-based evolutionary algorithm renowned for its robustness and efficiency in continuous parameter optimization, making it well-suited for this task.

3.3 Comparison Metrics

Four different evaluation metrics were used to measure the experimental results obtained by the applied methods and to perform a performance comparison.

3.3.1 PSNR

The system calculated the signal-to-noise ratio values between the original image and the watermarked image, as well as between the original watermark and the extracted watermark, according to Equation 1.

$$PSNR = 10\times\log_{10}\left(\frac{255^2}{\frac{1}{N\times N}\sum_{i=1}^{N}\sum_{j=1}^{N}[I_1(i,j)-I_2(i,j)]^2}\right) \tag{1}$$

In the equation:

$10\times\log_{10}$: This expression is used to calculate the ratio on a logarithmic scale. Multiplying by 10 converts the ratio into decibels (dB).

255 represents the maximum pixel value in an 8-bit image.

N represents the number of pixels along one dimension of the image.

$I_1(i,j)$ represents the pixel value at the ith row and jth column of the original image.

$I_2(i,j)$ represents the pixel value at the ith row and jth column of the reconstructed (watermarked) image.

PSNR is a significant metric used to evaluate the quality of digital images. It measures the similarity between an image and its altered version. Generally, it is used to determine the similarity between the original image and its processed version. A higher PSNR value indicates greater similarity between the images [15–17].

3.3.2 MSE

MSE is a metric used to evaluate how similar two signals are and calculated with Equation 2.

$$MSE = \frac{1}{mn}\sum_{i=0}^{m-1}\sum_{j=0}^{n-1}[I_1(i,j)-I_2(i,j)]^2 \tag{2}$$

In the equation:

$I_1(i,j)$ represents the pixel value at the i-th row and j-th column of the original image.

$I_2(i,j)$ represents the pixel value at the i-th row and j-th column of the reconstructed (watermarked) image.

m and n represent the dimensions of the image.

The MSE value ranges from 0 to ∞. A higher MSE indicates greater error and, consequently, lower image quality. Conversely, a lower MSE value signifies that the image is closer to the reference image and indicates better image quality [18].

3.3.3 SSIM

SSIM measures the similarity between two images. The SSIM value is derived from a combination of three factors: loss of correlation, luminance distortion, and contrast distortion. This metric reflects the structural similarity between images more effectively [16]. Unlike PSNR, SSIM takes into account luminance and contrast, providing a more accurate perceptual quality assessment. It yields more reliable results than PSNR, especially in cases involving structural distortions. The SSIM metric ranges from $[0,1]$ and is calculated using Equation 3. If the correlation between two images is low, the SSIM value approaches 0. A value of 1 indicates a high level of correlation. The positive

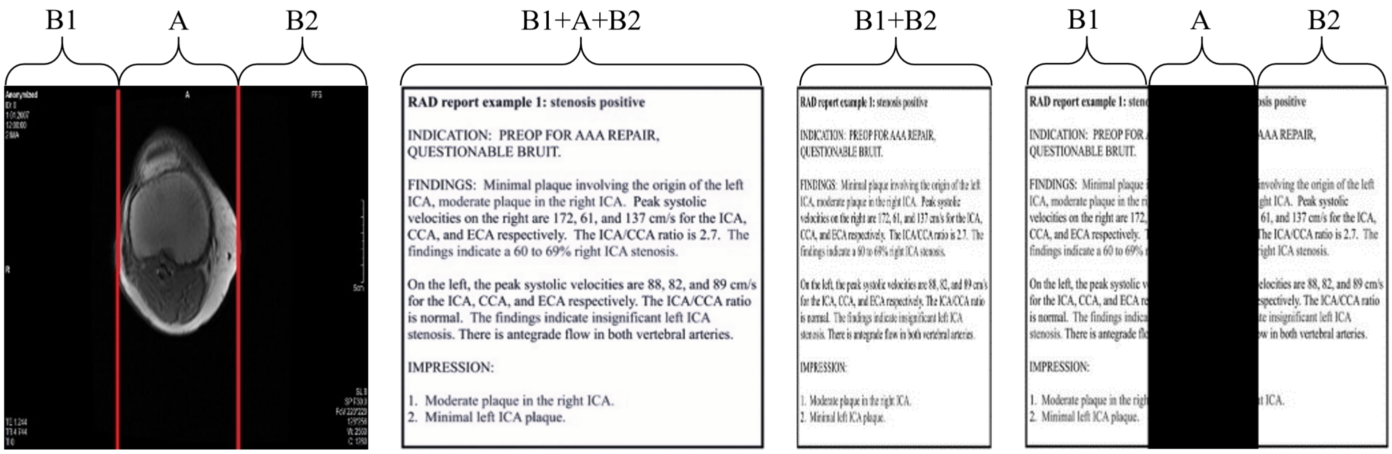

Figure 3. Representative illustration of the host image and the extracted watermark for the proposed method.

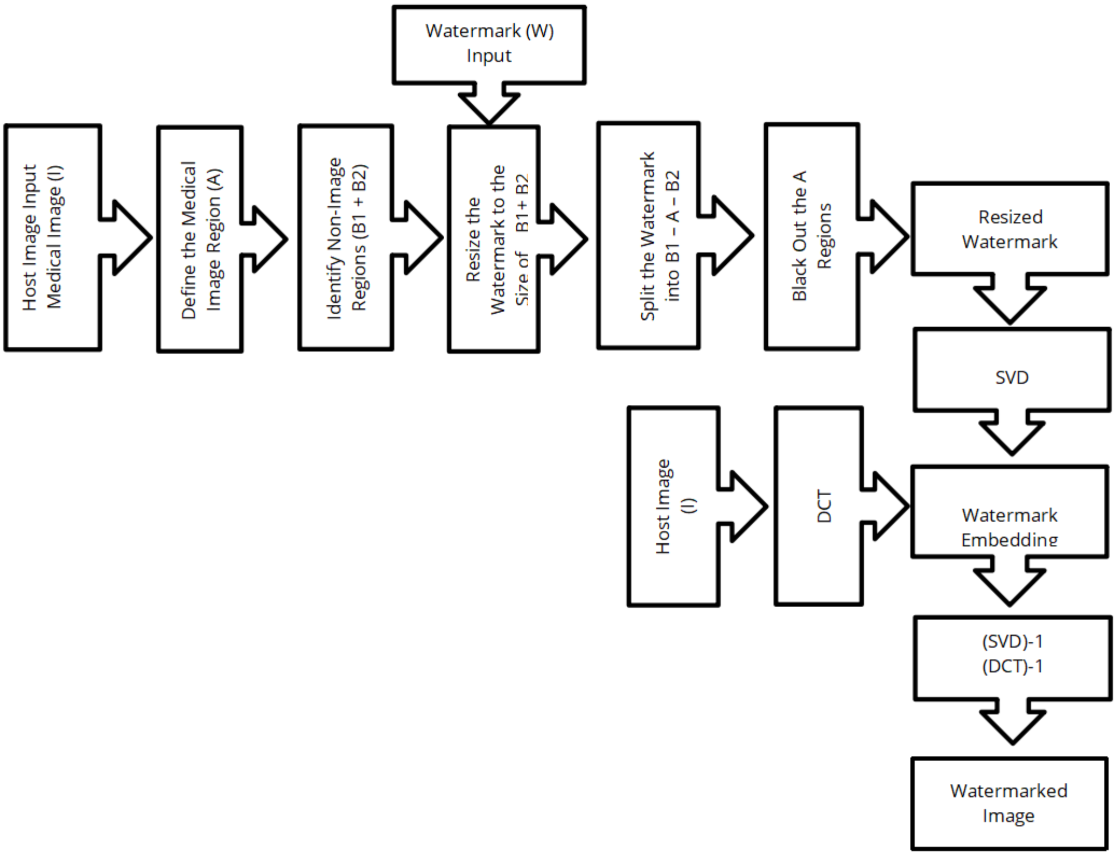

Figure 4. The diagram of the watermark embedding process for the proposed method (Method 3).

constants in Equation 4 (c1, c2, and c3) are used to prevent division by zero [16, 18, 19].

$$\mathrm{SSIM}(f,g) = I(f,g)c(f,g)s(f,g) \tag{3}$$

$$I(f,g) = \frac{2\mu_f\mu_g + c_1}{\mu_f^2 + \mu_g^2 + c_1} \tag{4}$$

$$c(f,g) = \frac{2\sigma_f\sigma_g + c_2}{\sigma_f^2 + \sigma_g^2 + c_2} \tag{5}$$

$$s(f,g) = \frac{\sigma_{fg} + c_3}{\sigma_f\sigma_g + c_3} \tag{6}$$

In Equation 4, the $I(f,g)$ is a luminance comparison function that compares the approximate brightness of two images (μ_f and μ_g). This factor reaches the value of 1 only when the two images are identical. The $c(f,g)$ is a contrast comparison function that evaluates the similarity of contrast between two images. Contrast is determined by the standard deviations σ_f and σ_g. When $\sigma_f = \sigma_g$, this term reaches its maximum value of

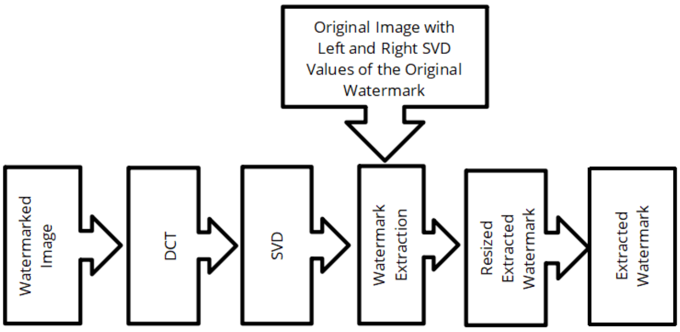

Figure 5. The block diagram of the watermark extraction process for the proposed method.

1. The $s(f, g)$ is a structure comparison function that measures the correlation coefficient between the two images [16, 18, 19].

3.3.4 NC

NC is a quantitative metric used to measure similarity. Therefore, it is used as an indicator of the effectiveness and robustness of watermarking algorithms. NC is calculated according to Equation 5 [2, 5].

$$NC = \frac{\sum_{x=0}^{M}\sum_{y=0}^{N} W(x,y) \cdot W'(x,y)}{\sqrt{\sum_{x=0}^{M}\sum_{y=0}^{N} W(x,y)^2} \cdot \sqrt{\sum_{x=0}^{M}\sum_{y=0}^{N} W'(x,y)^2}} \tag{7}$$

In this equation:

$W(x, y)$ represents the value at coordinates x and y of the original watermark.

$W'(x, y)$ represents the value at coordinates x and y of the extracted watermark.

M denotes the total number of pixels along the horizontal axis of the image.

N denotes the total number of pixels along the vertical axis of the image.

The NC value typically ranges between 0 and 1 when used to measure similarity between two images. This range indicates how similar the two images are. However, in cases of phase shift or negative correlation between images, the NC value can also take negative values. In general, a higher positive NC value indicates greater similarity, while a lower value suggests greater dissimilarity.

4 Experiments

In this study, patient reports were invisibly embedded into medical images using a DCT-SVD-based hybrid watermarking method, and three different strategies were evaluated. The fundamental processing steps are the same in all methods, with the difference being the location where the watermark is embedded. A non-blind watermarking structure was used, and the results were analyzed using PSNR, SSIM, MSE, and NC metrics, demonstrating that the proposed approach offers high visual quality and robustness.

4.1 Selection and Analysis of the Scaling Factor

In DCT-SVD-based watermarking methods, the selection of the scaling factor (SF) plays a critical role in both the quality of the host image and the robustness of the watermark [11]. As the scaling factor increases, the robustness of the watermark improves; however, this can lead to noticeable distortions in the original image [20]. Conversely, a lower scaling factor preserves the visual integrity of the host image but reduces the robustness of the watermark [14]. Therefore, determining this parameter at an optimal level is essential for the success of the watermarking system [21].

In the scope of this study, experiments were first conducted with different scaling values (ranging from -1 to 1). The obtained findings reveal the similarity between the watermarked and original images (IPSNR and ISSIM) as well as the similarity between the extracted and original watermark (WPSNR and WSSIM). After determining the optimal scaling factor (e.g., 0.01), the three different watermarking methods were evaluated using this fixed value, and the results were compared.

According to the obtained results, the proposed approach, namely the Segmented Watermark method, showed higher PSNR and SSIM values, especially at low scaling factors (0.01–0.05), compared to the other methods. At a scaling factor of 0.01, the IPSNR value was calculated as 44.47 and the ISSIM value as 0.9992. These values indicate high image quality and successful watermark integration. Similarly, the WPSNR and WSSIM metrics also show that the extracted watermark was obtained with high accuracy. The results of Tables 1, 2, 3, 4, 5, 6, 7, 8, 9 and Figure 6 confirm this.

The determination of the scaling factor is generally carried out using trial-and-error and experimental methods. Watermarked images are created using different scaling factors, and the effects of these factors on imperceptibility and confidentiality are examined. In the DCT-SVD-based hybrid watermarking technique, the scaling factor typically ranges between

Table 1. IPSNR, ISSIM, WPSNR and WSSIM values for Method 1 and W1 with different scaling factors.

SF	Method	Equal-Sized (Method 1) – W1 Block-Based Split Watermark (Proposed Method)												
	Image	I1	I2	I3	I4	I5	I6	I7	I8	I9	I10	I11	I12	I13
0.01	IPSNR	**40.374**	**40.550**	**40.549**	**40.521**	**40.469**	**40.456**	**41.117**	**40.402**	**40.422**	**40.391**	**40.424**	**40.433**	**40.403**
	WPSNR	34.684	**27.109**	**27.109**	**28.646**	**34.960**	**33.949**	**17.157**	38.085	39.659	43.737	**40.525**	42.644	44.855
	ISSIM	**0.997**	**0.994**	**0.994**	**0.995**	**0.994**	**0.990**	**0.953**	**0.983**	**0.985**	**0.991**	**0.999**	**0.995**	**0.992**
	WSSIM	0.955	**0.919**	**0.919**	**0.920**	**0.971**	**0.970**	**0.889**	0.973	0.979	0.987	**0.983**	0.989	0.989
0.03	IPSNR	30.899	31.101	31.101	31.075	30.999	31.008	31.670	30.899	30.910	30.901	30.949	30.899	30.899
	WPSNR	**44.003**	23.881	23.878	25.072	30.252	28.654	16.649	**47.118**	**43.584**	**48.308**	36.480	**50.939**	**50.073**
	ISSIM	0.989	0.956	0.956	0.960	0.957	0.942	0.826	0.927	0.933	0.945	0.992	0.965	0.951
	WSSIM	**0.991**	0.878	0.878	0.883	0.954	0.950	0.875	**0.994**	**0.989**	**0.996**	0.983	**0.997**	0.996
0.05	IPSNR	26.490	26.727	26.727	26.709	26.623	26.628	27.262	26.471	26.482	26.469	26.580	26.473	26.472
	WPSNR	26.490	22.193	22.190	23.028	26.769	25.722	16.579	45.603	41.110	47.007	30.840	48.436	48.715
	ISSIM	0.976	0.908	0.908	0.916	0.909	0.886	0.733	0.872	0.882	0.892	0.978	0.925	0.902
	WSSIM	**0.991**	0.851	0.851	0.854	0.921	0.921	0.877	**0.994**	0.988	**0.996**	0.965	**0.997**	**0.997**
0.1	IPSNR	20.638	20.868	20.868	20.868	20.779	20.737	21.339	20.491	20.494	20.455	20.851	20.595	20.528
	WPSNR	30.689	19.260	19.258	19.834	21.632	21.610	16.274	37.439	35.495	42.334	21.304	32.818	36.283
	ISSIM	0.933	0.798	0.798	0.811	0.799	0.7615	0.582	0.766	0.789	0.770	0.933	0.829	0.793
	WSSIM	0.976	0.789	0.789	0.805	0.842	0.8587	0.877	0.987	0.977	0.994	0.881	0.984	0.990
0.5	IPSNR	12.9505	8.933	8.933	9.136	8.824	8.439	8.868	9.226	8.423	7.211	9.804	9.049	8.624
	WPSNR	5.328	10.009	10.009	9.643	10.252	11.348	10.011	10.880	13.223	19.508	8.533	10.682	11.912
	ISSIM	0.640	0.357	0.357	0.367	0.359	0.329	0.240	0.365	0.381	0.360	0.607	0.422	0.390
	WSSIM	0.638	0.515	0.515	0.518	0.525	0.569	0.533	0.818	0.827	0.891	0.575	0.703	0.731
0.75	IPSNR	12.036	6.950	6.950	7.139	6.836	6.392	6.479	7.703	7.094	4.885	8.922	7.171	6.617
	WPSNR	3.637	7.653	7.652	7.387	7.791	8.535	7.858	7.345	8.281	13.010	5.624	7.803	8.688
	ISSIM	0.572	0.271	0.271	0.276	0.269	0.243	0.172	0.286	0.302	0.289	0.518	0.340	0.321
	WSSIM	0.482	0.486	0.486	0.486	0.484	0.502	0.429	0.716	0.737	0.751	0.487	0.616	0.629

Table 2. IPSNR, ISSIM, WPSNR and WSSIM values for Method 1 and W2 with different scaling factors

SF	Method	Equal-Sized (Method 1) – W2 Block-Based Split Watermark (Proposed Method)												
	Image	I1	I2	I3	I4	I5	I6	I7	I8	I9	I10	I11	I12	I13
0.01	IPSNR	**40.760**	**40.922**	**40.922**	**40.863**	**40.838**	**40.823**	**41.457**	**40.767**	**40.764**	**40.732**	**40.750**	**40.788**	**40.776**
	WPSNR	38.270	**26.940**	**26.942**	**28.789**	**35.087**	**33.498**	**17.547**	37.225	39.409	42.367	**40.245**	43.434	42.435
	ISSIM	**0.999**	**0.995**	**0.995**	**0.996**	**0.996**	**0.993**	**0.960**	**0.988**	**0.989**	**0.993**	**0.999**	**0.997**	**0.994**
	WSSIM	0.980	**0.926**	**0.926**	**0.931**	**0.980**	**0.968**	**0.909**	0.978	0.980	0.990	0.985	0.993	0.990
0.03	IPSNR	31.258	31.478	31.478	31.443	31.366	31.380	32.029	31.254	31.265	31.252	31.310	31.253	31.253
	WPSNR	**46.160**	23.678	23.676	24.956	29.943	28.148	16.914	**45.577**	**42.591**	**46.688**	35.999	**50.154**	**49.218**
	ISSIM	0.994	0.962	0.962	0.967	0.964	0.951	0.843	0.942	0.946	0.955	0.995	0.972	0.960
	WSSIM	**0.996**	0.884	0.884	0.896	0.900	0.944	0.889	0.995	**0.991**	0.996	**0.986**	**0.997**	0.997
0.05	IPSNR	26.840	27.115	27.115	27.087	26.995	27.006	27.626	26.826	26.838	26.825	26.825	26.825	26.823
	WPSNR	43.293	21.943	21.942	22.892	26.535	25.236	16.807	43.450	40.049	45.782	30.120	47.803	47.966
	ISSIM	0.987	0.920	0.920	0.929	0.921	0.899	0.754	0.881	0.900	0.908	0.985	0.939	0.918
	WSSIM	0.995	0.859	0.859	0.871	0.934	0.913	0.887	**0.996**	0.990	**0.996**	0.970	0.997	**0.997**
0.1	IPSNR	20.967	21.276	21.276	21.263	21.172	21.137	21.711	20.850	20.855	20.811	21.266	20.953	20.889
	WPSNR	31.936	18.939	18.938	19.651	21.400	21.144	16.424	36.068	34.363	40.845	20.780	32.948	35.609
	ISSIM	0.958	0.816	0.816	0.830	0.818	0.780	0.602	0.788	0.809	0.792	0.949	0.848	0.816
	WSSIM	0.984	0.803	0.803	0.821	0.865	0.855	0.879	0.989	0.984	0.993	0.902	0.988	0.990
0.5	IPSNR	13.092	9.308	9.307	9.513	9.234	8.859	9.337	9.436	8.650	7.594	10.131	9.406	8.998
	WPSNR	5.873	10.037	10.036	9.732	10.224	11.203	9.965	11.597	13.948	19.061	8.723	10.816	11.919
	ISSIM	0.702	0.374	0.374	0.385	0.376	0.344	0.247	0.372	0.391	0.372	0.649	0.440	0.409
	WSSIM	0.609	0.466	0.465	0.460	0.479	0.518	0.507	0.821	0.832	0.865	0.540	0.661	0.683
0.75	IPSNR	12.245	7.259	7.259	7.463	7.148	6.709	6.934	7.909	7.261	5.197	8.942	7.399	6.876
	WPSNR	4.086	7.868	7.868	7.606	7.981	8.670	7.896	7.897	8.907	13.059	6.135	8.172	8.989
	ISSIM	0.630	0.281	0.281	0.287	0.279	0.252	0.177	0.289	0.305	0.298	0.545	0.348	0.332
	WSSIM	0.436	0.418	0.418	0.412	0.418	0.429	0.374	0.697	0.725	0.683	0.425	0.553	0.563

-1 and 1 [7].

The PSNR and SSIM values between the original images and the watermarked images, as well as between the original watermarks and the extracted watermarks for different scaling factors, are presented in the tables for the medical images and watermarks used. The graphical representation of the PSNR values, obtained by selecting the I1 medical image and the W1

Table 3. IPSNR, ISSIM, WPSNR and WSSIM values for Method 2 and W1 with different scaling factors.

SF	Method	Block-Based (Method 2) – W1												
	Image	**I1**	**I2**	**I3**	**I4**	**I5**	**I6**	**I7**	**I8**	**I9**	**I10**	**I11**	**I12**	**I13**
0.01	IPSNR	**40.459**	**40.561**	**40.561**	**40.548**	**40.519**	**40.581**	**42.051**	**40.519**	**40.493**	**40.466**	**40.740**	**40.765**	**40.788**
	WPSNR	15.628	14.801	14.809	14.799	14.804	14.826	14.644	16.598	17.126	14.822	14.795	14.873	14.869
	ISSIM	**0.994**	**0.987**	**0.987**	**0.987**	**0.987**	**0.988**	**0.982**	**0.983**	**0.989**	**0.990**	**0.995**	**0.994**	**0.994**
	WSSIM	**0.715**	0.725	0.724	0.724	0.724	0.724	0.722	**0.656**	**0.589**	**0.725**	0.724	0.724	0.724
0.03	IPSNR	31.250	31.234	31.234	31.201	31.168	31.255	32.625	31.138	31.117	30.962	31.514	31.554	31.555
	WPSNR	15.906	15.110	15.112	15.107	15.108	15.155	14.817	16.863	17.038	15.163	15.186	15.217	15.214
	ISSIM	0.972	0.950	0.950	0.950	0.950	0.950	0.929	0.933	0.955	0.957	0.982	0.977	0.976
	WSSIM	0.712	**0.725**	**0.726**	**0.725**	**0.725**	**0.725**	**0.724**	0.651	0.576	0.724	**0.725**	**0.724**	**0.725**
0.05	IPSNR	26.972	26.971	26.971	26.930	26.889	27.020	28.226	26.782	26.765	26.542	27.335	27.361	27.360
	WPSNR	16.079	15.386	15.393	15.387	15.401	15.461	15.026	16.993	16.952	15.435	15.471	15.539	15.485
	ISSIM	0.948	0.916	0.916	0.917	0.917	0.914	0.885	0.885	0.917	0.922	0.971	0.958	0.956
	WSSIM	0.710	0.724	0.724	0.723	0.724	0.722	0.724	0.646	0.563	0.723	0.723	0.723	0.725
0.1	IPSNR	21.250	21.371	21.371	21.305	21.268	21.440	22.444	20.945	20.891	20.594	21.901	21.793	21.799
	WPSNR	16.424	16.135	16.149	16.136	16.144	16.205	15.415	17.214	16.714	16.143	16.248	16.287	16.268
	ISSIM	0.889	0.843	0.843	0.844	0.844	0.836	0.801	0.786	0.835	0.839	0.941	0.910	0.905
	WSSIM	0.706	0.718	0.718	0.718	0.717	0.716	0.723	0.640	0.541	0.718	0.714	0.714	0.715
0.5	IPSNR	12.182	9.527	9.527	9.480	9.527	9.509	10.755	9.188	8.785	8.284	10.749	10.129	10.082
	WPSNR	**17.352**	**16.728**	**16.719**	**16.750**	**16.766**	**16.744**	**17.637**	**16.698**	**16.291**	**16.759**	**16.735**	**16.682**	**16.635**
	ISSIM	0.607	0.508	0.508	0.511	0.512	0.494	0.480	0.404	0.432	0.486	0.690	0.597	0.585
	WSSIM	0.609	0.544	0.543	0.546	0.548	0.546	0.649	0.542	0.512	0.548	0.543	0.537	0.534
0.75	IPSNR	10.817	7.280	7.280	7.280	7.299	7.248	8.485	7.379	7.084	6.054	8.833	7.810	7.777
	WPSNR	16.673	16.401	16.384	16.398	16.395	16.460	17.126	16.411	16.291	16.393	16.403	16.300	16.291
	ISSIM	0.558	0.408	0.409	0.409	0.412	0.396	0.383	0.314	0.327	0.410	0.579	0.495	0.490
	WSSIM	0.540	0.519	0.518	0.520	0.520	0.522	0.575	0.525	0.512	0.519	0.519	0.513	0.512

Table 4. IPSNR, ISSIM, WPSNR and WSSIM values for Method 2 and W2 with different scaling factors.

SF	Method	Block-Based (Method 2) – W2												
	Image	**I1**	**I2**	**I3**	**I4**	**I5**	**I6**	**I7**	**I8**	**I9**	**I10**	**I11**	**I12**	**I13**
0.01	IPSNR	**40.907**	**40.949**	**40.950**	**40.941**	**40.911**	**40.977**	**42.462**	**40.910**	**40.866**	**40.848**	**41.156**	**41.155**	**41.171**
	WPSNR	14.961	13.717	13.719	13.732	13.766	13.781	13.763	15.454	**14.008**	13.808	13.812	13.874	13.861
	ISSIM	**0.995**	**0.989**	**0.989**	**0.989**	**0.989**	**0.990**	**0.986**	**0.986**	**0.992**	**0.992**	**0.995**	**0.995**	**0.995**
	WSSIM	**0.513**	**0.544**	**0.544**	**0.545**	**0.544**	**0.544**	0.537	**0.390**	**0.322**	**0.547**	**0.543**	**0.544**	**0.545**
0.03	IPSNR	31.629	31.644	31.644	31.610	31.576	31.660	33.042	31.522	31.501	31.357	31.915	31.939	31.938
	WPSNR	15.146	14.018	14.027	14.029	14.063	14.061	13.996	**15.468**	13.864	14.095	14.088	14.133	14.132
	ISSIM	0.978	0.956	0.956	0.956	0.956	0.955	0.938	0.941	0.963	0.962	0.983	0.979	0.978
	WSSIM	0.505	0.540	0.540	0.540	0.539	0.539	0.539	0.386	0.316	0.539	0.540	0.540	0.539
0.05	IPSNR	27.340	27.386	27.386	27.344	27.299	27.428	28.646	27.163	27.149	26.944	27.725	27.746	27.747
	WPSNR	15.301	14.221	14.231	14.220	14.248	14.269	14.183	15.414	13.727	14.262	**27.725**	14.334	14.326
	ISSIM	0.955	0.923	0.923	0.923	0.923	0.921	0.896	0.895	0.926	0.930	0.971	0.960	0.959
	WSSIM	0.493	0.536	0.536	0.534	0.535	0.532	**0.539**	0.382	0.311	0.534	0.532	0.530	0.532
0.1	IPSNR	21.619	21.807	21.807	21.740	21.694	21.866	22.858	21.320	21.277	21.000	22.319	22.194	22.200
	WPSNR	**15.469**	**14.576**	**14.578**	**14.566**	**14.623**	**14.673**	14.475	15.227	13.226	**14.653**	14.718	**14.780**	**14.773**
	ISSIM	0.900	0.851	0.851	0.851	0.851	0.844	0.814	0.796	0.844	0.850	0.940	0.912	0.908
	WSSIM	0.477	0.507	0.507	0.508	0.507	0.505	0.536	0.377	0.296	0.511	0.502	0.499	0.502
0.5	IPSNR	12.416	9.938	9.938	9.895	9.935	9.930	11.261	9.510	9.114	8.648	11.221	10.566	10.516
	WPSNR	14.555	12.440	12.426	12.459	12.485	12.223	**14.751**	13.061	12.042	12.394	12.113	12.086	12.092
	ISSIM	0.619	0.512	0.512	0.516	0.515	0.497	0.487	0.400	0.423	0.486	0.685	0.593	0.579
	WSSIM	0.360	0.277	0.276	0.278	0.281	0.265	0.372	0.285	0.245	0.277	0.252	0.251	0.250
0.75	IPSNR	11.052	7.628	7.628	7.628	7.662	7.635	8.958	7.629	7.315	6.433	9.154	8.196	8.168
	WPSNR	12.968	12.105	12.092	12.162	12.189	12.055	13.756	12.467	12.042	12.139	12.042	12.042	12.042
	ISSIM	0.567	0.406	0.406	0.408	0.410	0.393	0.385	0.306	0.317	0.402	0.577	0.488	0.480
	WSSIM	0.282	0.249	0.248	0.253	0.255	0.246	0.319	0.265	0.245	0.252	0.245	0.245	0.245

watermark, is provided in Figure 7. When the other results are examined, it is observed that changes in the scaling factor do not affect the performance ranking of the methods across different images, nor does the choice of image alter this ranking.

To analyze Figure 7 in detail, the PSNR variations for each scaling factor are examined. The graph

Table 5. IPSNR, ISSIM, WPSNR and WSSIM values for Method 3 and W1 with different scaling factors.

SF	Method	Segmented Watermark (Method 3) – W1												
	Image	**I1**	**I2**	**I3**	**I4**	**I5**	**I6**	**I7**	**I8**	**I9**	**I10**	**I11**	**I12**	**I13**
0.01	IPSNR	**44.465**	**42.706**	**42.705**	**42.747**	**42.698**	**42.905**	**43.921**	**42.532**	**43.295**	**44.097**	**42.797**	**42.470**	**42.549**
	WPSNR	27.932	**28.745**	**28.757**	**30.269**	**37.053**	**36.319**	**17.505**	36.405	39.494	38.812	38.404	40.786	41.842
	ISSIM	**0.999**	**0.997**	**0.997**	**0.997**	**0.997**	**0.995**	**0.970**	**0.989**	**0.990**	**0.996**	**0.999**	**0.998**	**0.995**
	WSSIM	0.969	**0.915**	**0.914**	**0.919**	**0.969**	**0.974**	**0.889**	0.965	0.976	0.970	0.980	0.985	0.986
0.03	IPSNR	34.678	33.304	33.304	33.342	33.279	33.497	34.529	33.029	33.834	34.664	33.259	33.012	33.040
	WPSNR	43.925	24.963	24.964	26.224	32.218	30.607	16.782	**47.779**	**46.218**	47.932	**38.813**	**51.761**	50.871
	ISSIM	0.994	0.970	0.970	0.973	0.971	0.962	0.875	0.945	0.954	0.971	0.995	0.975	0.965
	WSSIM	0.993	0.878	0.878	0.892	0.966	0.962	0.868	0.995	**0.994**	0.996	**0.989**	0.997	0.997
0.05	IPSNR	30.246	28.921	28.921	28.955	28.891	29.104	30.120	28.594	29.408	30.239	28.859	28.582	28.608
	WPSNR	**45.451**	23.313	23.314	24.367	28.894	27.795	16.687	47.541	43.994	**49.840**	34.541	51.503	**51.029**
	ISSIM	0.988	0.935	0.934	0.942	0.936	0.920	0.794	0.899	0.916	0.937	0.986	0.947	0.927
	WSSIM	**0.995**	0.851	0.851	0.866	0.943	0.940	0.869	**0.996**	0.993	**0.998**	0.981	**0.998**	**0.998**
0.1	IPSNR	24.270	23.014	23.014	23.061	22.991	23.177	24.155	22.594	23.404	24.225	23.015	22.614	22.610
	WPSNR	40.954	20.763	20.761	21.441	23.949	23.743	16.585	41.298	39.364	47.696	25.121	40.255	44.012
	ISSIM	0.962	0.844	0.844	0.857	0.847	0.818	0.653	0.808	0.839	0.851	0.955	0.868	0.836
	WSSIM	0.994	0.805	0.805	0.819	0.879	0.886	0.872	0.993	0.988	0.997	0.925	0.994	0.996
0.5	IPSNR	14.110	10.422	10.422	10.633	10.395	10.272	11.082	10.393	10.262	10.307	11.199	10.454	10.148
	WPSNR	8.456	11.742	11.742	11.448	12.152	13.651	12.178	13.930	18.781	32.642	10.269	12.732	14.174
	ISSIM	0.720	0.428	0.428	0.441	0.434	0.404	0.306	0.425	0.475	0.462	0.678	0.484	0.447
	WSSIM	0.777	0.499	0.499	0.506	0.522	0.602	0.624	0.865	0.876	0.974	0.584	0.739	0.781
0.75	IPSNR	13.013	8.135	8.135	8.368	8.040	7.739	8.328	8.563	7.361	9.273	8.197	7.719	13.013
	WPSNR	5.520	9.261	9.261	8.955	9.548	10.780	9.863	9.322	20.995	7.660	9.589	10.772	5.520
	ISSIM	0.641	0.318	0.318	0.328	0.320	0.297	0.223	0.331	0.365	0.562	0.380	0.356	0.641
	WSSIM	0.639	0.478	0.478	0.479	0.480	0.519	0.473	0.781	0.905	0.520	0.651	0.679	0.639

Table 6. IPSNR, ISSIM, WPSNR and WSSIM values for Method 3 and W2 with different scaling factors.

SF	Method	Segmented Watermark (Method 3) – W2												
	Image	**I1**	**I2**	**I3**	**I4**	**I5**	**I6**	**I7**	**I8**	**I9**	**I10**	**I11**	**I12**	**I13**
0.01	IPSNR	**44.432**	**42.689**	**42.690**	**42.731**	**42.682**	**42.892**	**43.905**	**42.863**	**43.626**	**44.429**	**43.146**	**42.822**	**42.864**
	WPSNR	28.189	28.764	28.760	30.363	**37.218**	**36.295**	17.514	34.977	36.571	36.754	**38.680**	39.302	41.519
	ISSIM	**0.999**	**0.996**	**0.996**	**0.997**	**0.997**	**0.995**	**0.970**	**0.992**	**0.992**	**0.998**	**0.999**	**0.998**	**0.997**
	WSSIM	0.967	**0.911**	**0.911**	**0.923**	0.967	**0.974**	0.891	0.967	0.973	0.976	0.987	0.985	0.987
0.03	IPSNR	35.018	33.687	33.687	33.715	33.647	33.872	34.892	33.382	34.192	35.031	33.622	33.365	33.391
	WPSNR	**43.704**	24.645	24.644	26.071	31.865	30.032	17.048	**47.446**	**44.691**	**47.165**	38.434	**50.898**	**50.424**
	ISSIM	0.997	0.975	0.975	0.978	0.976	0.968	0.891	0.957	0.965	0.978	0.997	0.980	0.973
	WSSIM	0.994	0.901	0.902	0.915	**0.972**	0.961	**0.900**	0.996	**0.994**	0.997	**0.990**	0.998	0.997
0.05	IPSNR	30.601	29.309	29.309	29.336	29.266	29.480	30.486	28.949	29.764	30.593	29.228	28.936	28.962
	WPSNR	29.336	**29.266**	**29.480**	**30.486**	28.949	29.764	**30.593**	29.228	28.936	28.962	29.336	29.266	29.480
	ISSIM	0.994	0.944	0.944	0.951	0.946	0.931	0.813	0.917	0.932	0.949	0.991	0.957	0.941
	WSSIM	**0.998**	0.877	0.877	0.889	0.954	0.938	0.898	**0.997**	0.993	**0.997**	0.983	**0.998**	**0.998**
0.1	IPSNR	24.619	23.420	23.420	23.456	23.379	23.572	24.523	22.954	23.764	24.581	23.419	22.971	22.968
	WPSNR	41.825	20.375	20.374	21.201	23.663	23.158	16.771	39.192	37.864	46.261	24.225	40.264	43.247
	ISSIM	0.981	0.861	0.861	0.874	0.864	0.836	0.675	0.830	0.859	0.872	0.967	0.885	0.858
	WSSIM	0.996	0.831	0.831	0.844	0.903	0.887	0.891	0.994	0.990	0.997	0.937	0.995	0.996
0.5	IPSNR	14.286	10.853	10.853	11.056	10.849	10.718	11.542	10.632	10.589	10.675	11.646	10.873	10.551
	WPSNR	9.142	11.560	11.560	11.382	11.945	13.334	12.039	14.742	19.101	30.424	10.196	12.684	14.019
	ISSIM	0.782	0.449	0.449	0.464	0.454	0.422	0.315	0.440	0.493	0.480	0.719	0.507	0.471
	WSSIM	0.780	0.476	0.476	0.468	0.505	0.578	0.618	0.881	0.890	0.964	0.583	0.723	0.754
0.75	IPSNR	13.162	8.480	8.483	8.732	8.428	8.138	8.816	8.765	7.751	9.494	8.501	8.051	13.162
	WPSNR	6.072	9.361	9.361	9.082	9.575	10.690	9.772	9.976	20.363	8.005	9.841	10.917	6.072
	ISSIM	0.708	0.334	0.334	0.345	0.337	0.312	0.231	0.341	0.379	0.604	0.398	0.373	0.708
	WSSIM	0.618	0.422	0.422	0.415	0.428	0.462	0.449	0.774	0.886	0.475	0.601	0.626	0.618

compares the PSNR values of three different methods (Equal-Sized, Block-Based, and Segmented Watermark (Method 3)) on the I1 image. For a scaling factor of 0.01:

- PSNR_I (Equal-Sized): 40.374
- PSNR_W (Equal-Sized): 34.684
- PSNR_I (Block-Based): 40.460

Table 7. Results obtained for both watermarks using a 0.01 scaling factor according to Method 1.

Image	W1								W2							
	PSNR_I	PSNR_W	MSE_I	MSE_W	SSIM_I	SSIM_W	NC_I	NC_W	PSNR_I	PSNR_W	MSE_I	MSE_W	SSIM_I	SSIM_W	NC_I	NC_W
I1	40.374	34.684	9.174e-5	3.400e-4	0.997	0.955	0.999	0.994	40.760	38.270	8.393e-5	1.489e-4	0.999	0.980	0.999	0.998
I2	40.550	27.109	8.810e-5	1.945e-4	0.994	0.919	0.999	0.983	40.922	26.940	8.086e-5	2.023e-3	0.995	0.926	0.999	0.991
I3	40.549	27.109	8.810e-5	1.945e-4	0.994	0.919	0.999	0.983	40.922	26.942	8.086e-5	2.021e-3	0.995	0.926	0.999	0.991
I4	40.521	28.646	8.868e-5	1.365e-3	0.995	0.920	0.999	0.987	40.863	28.789	8.196e-5	1.321e-3	0.996	0.931	0.999	0.993
I5	40.469	34.960	8.976e-5	3.191e-4	0.994	0.971	0.999	0.997	40.838	35.087	8.244e-5	3.099e-4	0.996	0.980	0.999	0.998
I6	40.456	33.949	9.001e-5	4.027e-4	0.990	0.970	0.999	0.997	40.823	33.498	8.272e-5	4.468e-4	0.993	0.968	0.999	0.998
I7	41.117	17.157	7.730e-5	1.924e-2	0.953	0.889	0.999	0.979	41.457	17.547	7.149e-5	1.759e-2	0.960	0.909	0.999	0.991
I8	40.402	38.085	9.113e-5	1.554e-4	0.983	0.973	0.999	0.997	40.767	37.225	8.380e-5	1.894e-4	0.988	0.978	0.999	0.998
I9	40.422	39.659	9.072e-5	1.081e-4	0.985	0.979	0.999	0.998	40.764	39.409	8.385e-5	1.145e-4	0.989	0.980	0.999	0.999
I10	40.391	43.737	9.137e-5	4.229e-5	0.991	0.987	0.999	0.999	40.732	42.367	8.447e-5	5.797e-5	0.993	0.990	0.999	0.999
I11	40.424	40.525	9.068e-5	8.861e-5	0.999	0.983	0.999	0.998	40.750	40.245	8.413e-5	9.451e-5	0.999	0.985	0.999	0.999
I12	40.433	42.644	9.049e-5	5.439e-5	0.995	0.989	0.999	0.999	40.7884	43.434	8.339e-5	4.534e-5	0.997	0.993	0.999	0.999
I13	40.403	44.855	9.112e-5	3.269e-5	0.992	0.989	0.999	0.999	40.7762	42.435	8.363e-5	5.707e-5	0.994	0.990	0.999	0.999

Table 8. Results obtained for both watermarks using a 0.01 scaling factor according to Method 2.

Image	W1								W2							
	PSNR_I	PSNR_W	MSE_I	MSE_W	SSIM_I	SSIM_W	NC_I	NC_W	PSNR_I	PSNR_W	MSE_I	MSE_W	SSIM_I	SSIM_W	NC_I	NC_W
I1	40.459	15.628	8.995e-5	17.696	0.994	0.715	0.999	0.802	40.907	14.961	8.113e-5	24.427	0.995	0.513	0.999	0.804
I2	40.561	14.801	8.787e-5	20.886	0.987	0.725	0.999	0.810	40.949	13.717	8.035e-5	30.404	0.989	0.544	0.999	0.780
I3	40.561	14.809	8.787e-5	20.840	0.987	0.724	0.999	0.810	40.950	13.719	8.035e-5	30.373	0.989	0.544	0.999	0.780
I4	40.548	14.799	8.814e-5	20.824	0.987	0.724	0.999	0.809	40.941	13.732	8.050e-5	30.311	0.989	0.545	0.999	0.780
I5	40.519	14.804	8.872e-5	20.855	0.987	0.724	0.999	0.810	40.911	13.766	8.106e-5	30.233	0.989	0.544	0.999	0.782
I6	40.581	14.826	8.747e-5	20.762	0.988	0.724	0.999	0.809	40.977	13.781	7.985e-5	30.279	0.990	0.544	0.999	0.783
I7	42.051	14.644	6.235e-5	21.805	0.982	0.722	0.999	0.819	42.462	13.763	5.672e-5	32.614	0.986	0.537	0.999	0.805
I8	40.519	16.598	8.873e-5	11.828	0.983	0.656	0.999	0.720	40.910	15.454	8.108e-5	15.295	0.986	0.390	0.999	0.769
I9	40.493	17.126	8.926e-5	4.2023	0.989	0.589	0.999	0.523	40.866	14.008	8.191e-5	7.300	0.992	0.322	0.999	0.613
I10	40.466	14.822	8.982e-5	20.855	0.990	0.725	0.999	0.812	40.848	13.808	8.225e-5	30.388	0.992	0.547	0.999	0.786
I11	40.740	14.795	8.433e-5	20.980	0.995	0.724	0.999	0.812	41.156	13.812	7.662e-5	30.357	0.995	0.543	0.999	0.786
I12	40.765	14.873	8.384e-5	20.653	0.994	0.724	0.999	0.811	41.155	13.874	7.664e-5	30.139	0.995	0.544	0.999	0.788
I13	40.788	14.869	8.339e-5	20.684	0.994	0.724	0.999	0.811	41.171	13.861	7.636e-5	30.062	0.995	0.545	0.999	0.787

Table 9. Results obtained for both watermarks using a 0.01 scaling factor according to Method 3.

Image	W1								W2							
	PSNR_I	PSNR_W	MSE_I	MSE_W	SSIM_I	SSIM_W	NC_I	NC_W	PSNR_I	PSNR_W	MSE_I	MSE_W	SSIM_I	SSIM_W	NC_I	NC_W
I1	44.465	27.932	3.576e-5	1.609e-3	0.999	0.969	0.999	0.996	44.432	28.189	3.603e-5	1.517e-3	0.999	0.967	1	0.998
I2	42.706	28.745	5.362e-5	1.334e-3	0.997	0.915	0.999	0.984	42.689	28.764	5.382e-5	1.329e-3	0.996	0.911	0.999	0.992
I3	42.705	28.757	5.363e-5	1.331e-3	0.997	0.914	0.999	0.984	42.690	28.760	5.382e-5	1.330e-3	0.996	0.911	0.999	0.992
I4	42.747	30.269	5.311e-5	9.399e-4	0.997	0.919	0.999	0.987	42.731	30.363	5.331e-5	9.196e-4	0.997	0.923	0.999	0.995
I5	42.698	37.053	5.372e-5	1.970e-4	0.997	0.969	0.999	0.996	42.682	37.218	5.391e-5	1.897e-4	0.997	0.967	0.999	0.998
I6	42.905	36.319	5.121e-5	2.333e-4	0.995	0.974	0.999	0.997	42.892	36.295	5.137e-5	2.346e-4	0.995	0.974	0.999	0.998
I7	43.921	17.505	4.053e-5	1.776e-2	0.970	0.889	0.999	0.977	43.905	17.514	4.069e-5	1.772e-2	0.970	0.891	0.999	0.988
I8	42.532	36.405	5.581e-5	2.287e-4	0.989	0.965	0.999	0.996	42.863	34.977	5.172e-5	3.178e-4	0.992	0.967	0.999	0.997
I9	43.295	39.494	4.682e-5	1.123e-4	0.990	0.976	0.999	0.998	43.626	36.571	4.338e-5	2.202e-4	0.992	0.973	0.999	0.998
I10	44.097	38.812	3.893e-5	1.314e-4	0.996	0.970	0.999	0.997	44.429	36.754	3.606e-5	2.111e-4	0.998	0.976	0.999	0.998
I11	42.797	38.404	5.251e-5	1.443e-4	0.999	0.980	0.999	0.998	43.146	38.680	4.846e-5	1.355e-4	0.999	0.987	0.999	0.999
I12	42.470	40.786	5.661e-5	8.343e-5	0.998	0.985	0.999	0.998	42.822	39.302	5.220e-5	1.174e-4	0.998	0.985	0.999	0.999
I13	42.549	41.842	5.560e-5	6.542e-5	0.995	0.986	0.999	0.999	42.864	41.519	5.170e-5	7.048e-5	0.997	0.987	0.999	0.999

- PSNR_W (Block-Based): 15.629
- PSNR_I (Segmented Watermark (Method 3)): 44.466
- PSNR_W (Segmented Watermark (Method 3)): 27.932

The Segmented Watermark (Method 3) achieves higher values in both PSNR_I and PSNR_W metrics compared to the other methods, indicating high image quality and high watermark quality. For a scaling factor of 0.03:

- PSNR_I (Equal-Sized): 30.899
- PSNR_W (Equal-Sized): 44.003
- PSNR_I (Block-Based): 31.251
- PSNR_W (Block-Based): 15.907
- PSNR_I (Segmented Watermark (Method 3)): 34.679
- PSNR_W (Segmented Watermark (Method 3)): 43.926

The Segmented Watermark (Method 3) again demonstrates superiority in both PSNR_I and PSNR_W, with PSNR_I significantly higher than the other methods. For a scaling factor of 0.05:

- PSNR_I (Equal-Sized): 26.491
- PSNR_W (Equal-Sized): 26.491
- PSNR_I (Block-Based): 26.973
- PSNR_W (Block-Based): 16.079
- PSNR_I (Segmented Watermark (Method 3)): 30.247

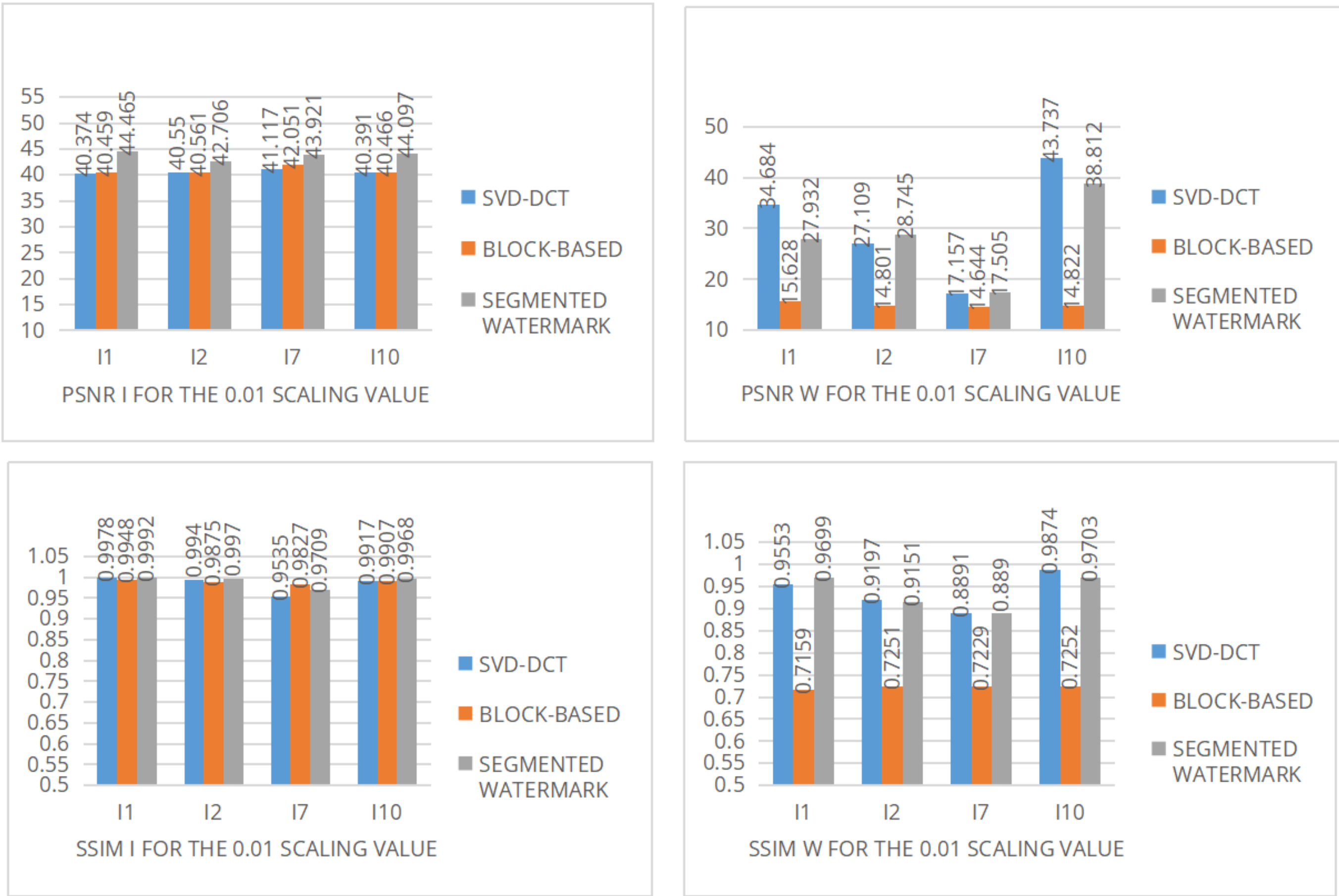

Figure 6. Graph of the variations in IPSNR, ISSIM, WPSNR and WSSIM for images I1, I2, I7, and I10 using a 0.01 scaling factor.

- PSNR_W (Segmented Watermark (Method 3)): 45.451

The Segmented Watermark (Method 3) performs particularly well in PSNR_W and also achieves higher PSNR_I than the other methods. For a scaling factor of 0.1:

- PSNR_I (Equal-Sized): 20.639
- PSNR_W (Equal-Sized): 30.690
- PSNR_I (Block-Based): 21.251
- PSNR_W (Block-Based): 16.425
- PSNR_I (Segmented Watermark (Method 3)): 24.271
- PSNR_W (Segmented Watermark (Method 3)): 40.954

Again, the Segmented Watermark (Method 3) yields higher PSNR_I and PSNR_W values than the other methods. For a scaling factor of 0.5:

- PSNR_I (Equal-Sized): 12.951
- PSNR_W (Equal-Sized): 5.329
- PSNR_I (Block-Based): 12.182
- PSNR_W (Block-Based): 17.353
- PSNR_I (Segmented Watermark (Method 3)): 14.111
- PSNR_W (Segmented Watermark (Method 3)): 8.457

Although the Block-Based method shows higher PSNR_W, the Segmented Watermark (Method 3) provides a more balanced performance with higher PSNR_I overall. For a scaling factor of 0.75:

- PSNR_I (Equal-Sized): 12.037
- PSNR_W (Equal-Sized): 3.637
- PSNR_I (Block-Based): 10.818
- PSNR_W (Block-Based): 16.673
- PSNR_I (Segmented Watermark (Method 3)): 13.013

- PSNR_W (Segmented Watermark (Method 3)): 5.520

Again, the Block-Based method achieves higher PSNR_W, but the Segmented Watermark (Method 3) performs better in PSNR_I.

Overall, analyzing Figure 7, it can be concluded that the Segmented Watermark (Method 3) outperforms the other methods in both image quality (PSNR_I) and extracted watermark quality (PSNR_W). Especially at low scaling factors (0.01, 0.03, 0.05), the Segmented Watermark (Method 3) demonstrates significantly better performance. As the scaling factor increases (0.5 and 0.75), the difference with other methods decreases, but the Segmented Watermark (Method 3) still maintains high PSNR_I values.

The graphical representation of the SSIM values, obtained by selecting the I1 medical image and the W1 watermark, is provided in Figure 8. Examining the SSIM variations for each scaling factor, the graph compares three different methods (Equal-Sized, Block-Based, and Segmented Watermark (Method 3)) on the I1 image. For a scaling factor of 0.01:

- SSIM_I (Equal-Sized): 0.99782
- SSIM_W (Equal-Sized): 0.95539
- SSIM_I (Block-Based): 0.99489
- SSIM_W (Block-Based): 0.71593
- SSIM_I (Segmented Watermark (Method 3)): 0.99922
- SSIM_W (Segmented Watermark (Method 3)): 0.96998

The Segmented Watermark (Method 3) achieves higher values in both SSIM_I and SSIM_W, indicating high image similarity and high watermark quality. For a scaling factor of 0.03:

- SSIM_I (Equal-Sized): 0.98784
- SSIM_W (Equal-Sized): 0.99144
- SSIM_I (Block-Based): 0.97290
- SSIM_W (Block-Based): 0.71729
- SSIM_I (Segmented Watermark (Method 3)): 0.99436
- SSIM_W (Segmented Watermark (Method 3)): 0.99378

The Segmented Watermark (Method 3) again demonstrates superiority, especially in SSIM_W. For a scaling factor of 0.05:

- SSIM_I (Equal-Sized): 0.97668
- SSIM_W (Equal-Sized): 0.99149
- SSIM_I (Block-Based): 0.94884
- SSIM_W (Block-Based): 0.71012
- SSIM_I (Segmented Watermark (Method 3)): 0.98842
- SSIM_W (Segmented Watermark (Method 3)): 0.99597

The Segmented Watermark (Method 3) achieves very high SSIM_W and also superior SSIM_I values. For a scaling factor of 0.1:

- SSIM_I (Equal-Sized): 0.93397
- SSIM_W (Equal-Sized): 0.97662
- SSIM_I (Block-Based): 0.88909
- SSIM_W (Block-Based): 0.70614
- SSIM_I (Segmented Watermark (Method 3)): 0.96274
- SSIM_W (Segmented Watermark (Method 3)): 0.99490

Again, the Segmented Watermark (Method 3) shows higher SSIM_I and SSIM_W than the other methods. For a scaling factor of 0.5:

- SSIM_I (Equal-Sized): 0.64047
- SSIM_W (Equal-Sized): 0.63839
- SSIM_I (Block-Based): 0.60779
- SSIM_W (Block-Based): 0.60925
- SSIM_I (Segmented Watermark (Method 3)): 0.72036
- SSIM_W (Segmented Watermark (Method 3)): 0.77700

Although the Equal-Sized method shows higher SSIM_W, the Segmented Watermark (Method 3) provides a more balanced performance and higher SSIM_I overall. For a scaling factor of 0.75:

- SSIM_I (Equal-Sized): 0.57220
- SSIM_W (Equal-Sized): 0.48215
- SSIM_I (Block-Based): 0.55811

- SSIM_W (Block-Based): 0.54041
- SSIM_I (Segmented Watermark (Method 3)): 0.64186
- SSIM_W (Segmented Watermark (Method 3)): 0.63976

The Block-Based method achieves higher SSIM_W, but the Segmented Watermark (Method 3) performs better in SSIM_I. Considering Tables 1, 2, 3, 4, 5, 6, 7, 8, 9 and Figures 6, 7, 8 to determine the optimal scaling range, it is clear that the most suitable range is between 0.01 and 0.05, where high image quality and watermark quality are balanced. More specifically:

- Scaling factor 0.01: Highest image quality with good watermark quality
- Scaling factor 0.03: Balanced and high quality
- Scaling factor 0.05: High watermark quality with acceptable image quality

Therefore, 0.01 and 0.03 appear particularly optimal, as in this range, image and watermark quality are most effectively balanced. As the scaling factor increases, especially beyond 0.1, a noticeable decrease in image quality is observed, indicating that values above 0.1 are not suitable for watermarking. Thus, the ideal range for watermarking operations can be considered between 0.01 and 0.05, with 0.01 being the most optimal value within this range.

As a result of the analysis, it was determined that the scaling factor range between 0.01 and 0.05 is the most suitable. Within this range, an ideal balance between image quality and watermark quality can be achieved. When the scaling factor is selected as 0.01, it was observed that the proposed method provides both high-quality host images and robust watermark extraction.

4.2 Analysis of the Results of Compared Methods

In line with the conducted analyses, when different scaling factors were examined, significant quality degradation was observed in both the host image and the extracted watermark, especially for values of 0.1 and above. Therefore, the range between 0.01 and 0.05 was evaluated as the most suitable interval in terms of both image and watermark quality. In particular, the 0.01 scaling factor stood out as the ideal value, minimizing image distortion while preserving watermark extractability.

Method 1 is based on using the host and watermark images in the same size. In this method, the quality of the original image remains high, and the visual similarity yields quite successful results. However, the quality of the extracted watermark is not always consistent.

Method 2 presents a block-based approach in which the host image is divided into smaller regions for processing. In this structure, distortion in the host image is quite low; however, the quality of the watermark is significantly reduced. In many cases, the extracted watermarks show low similarity.

The proposed Method 3 is based on embedding the watermark into the non-informative regions of the medical images. Thanks to this strategy, the essential parts of the host image are preserved, and high quality is achieved in both the host and watermark images. In terms of visual similarity (SSIM) and distortion measurements (PSNR, MSE), Method 3 has shown consistent and superior performance compared to the other two methods.

Overall, Method 3 stands out as the most appropriate approach for secure and invisible watermarking in medical images by providing the best balance between image and watermark quality. Especially in scenarios where patient privacy is critical, this method is recommended.

The superiority of the proposed Method 3 can be attributed to its selective embedding strategy. By targeting non-informative regions of medical images, the method avoids altering diagnostically significant pixels. This selective embedding minimizes pixel-level differences between the original and watermarked images, leading to higher PSNR values. Moreover, structural similarities are preserved in informative regions, resulting in higher SSIM values. Unlike Method 1 and Method 2, where watermark embedding may interfere with critical regions or be diluted across blocks, Method 3 ensures that the watermark is robustly embedded without compromising image quality. Consequently, both the host image and the extracted watermark maintain high fidelity, demonstrating the effectiveness of segmenting non-informative regions for watermark embedding.

4.3 Discussion and Conclusion

To evaluate the robustness of the proposed Method 3, various types of attacks were applied and the resulting watermark quality metrics were analyzed. Common digital attacks such as rotation, salt-and-pepper noise, JPEG compression, and sharpening were considered

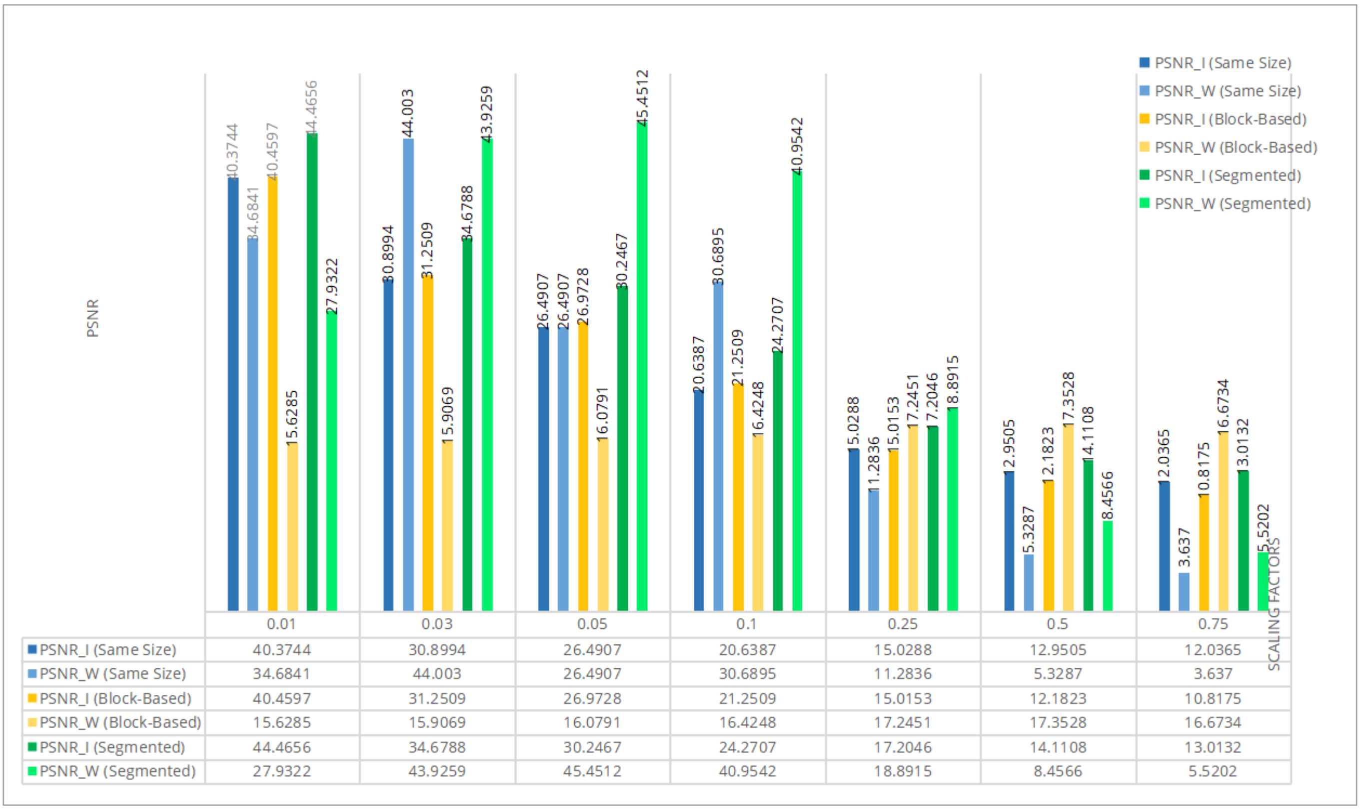

	0.01	0.03	0.05	0.1	0.25	0.5	0.75
PSNR_I (Same Size)	40.3744	30.8994	26.4907	20.6387	15.0288	12.9505	12.0365
PSNR_W (Same Size)	34.6841	44.003	26.4907	30.6895	11.2836	5.3287	3.637
PSNR_I (Block-Based)	40.4597	31.2509	26.9728	21.2509	15.0153	12.1823	10.8175
PSNR_W (Block-Based)	15.6285	15.9069	16.0791	16.4248	17.2451	17.3528	16.6734
PSNR_I (Segmented)	44.4656	34.6788	30.2467	24.2707	17.2046	14.1108	13.0132
PSNR_W (Segmented)	27.9322	43.9259	45.4512	40.9542	18.8915	8.4566	5.5202

Figure 7. PSNR variation according to scaling factors for I1.

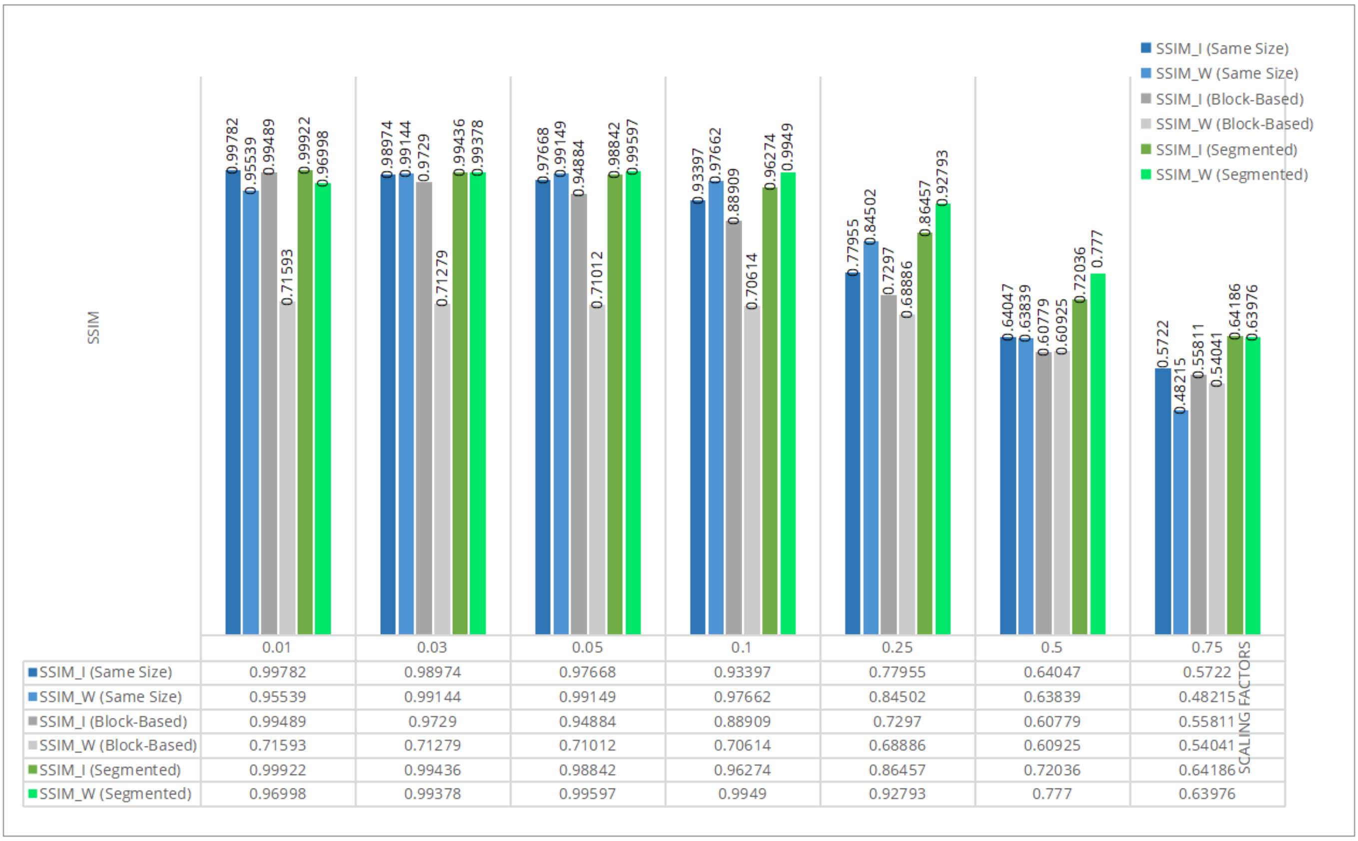

	0.01	0.03	0.05	0.1	0.25	0.5	0.75
SSIM_I (Same Size)	0.99782	0.98974	0.97668	0.93397	0.77955	0.64047	0.5722
SSIM_W (Same Size)	0.95539	0.99144	0.99149	0.97662	0.84502	0.63839	0.48215
SSIM_I (Block-Based)	0.99489	0.9729	0.94884	0.88909	0.7297	0.60779	0.55811
SSIM_W (Block-Based)	0.71593	0.71279	0.71012	0.70614	0.68886	0.60925	0.54041
SSIM_I (Segmented)	0.99922	0.99436	0.98842	0.96274	0.86457	0.72036	0.64186
SSIM_W (Segmented)	0.96998	0.99378	0.99597	0.9949	0.92793	0.777	0.63976

Figure 8. SSIM variation according to scaling factors for I1.

in this analysis. The evaluations were carried out on watermarked medical images obtained with a scaling factor of 0.01. Following the rotation attack, partial degradation in watermark quality was observed.

While a decrease was noted in metrics such as PSNR and SSIM, NC values also declined. This indicates that the rotation operation negatively affects the structural integrity of the watermark. When salt-and-pepper noise was added, a significant quality loss occurred in both the host image and the watermark. The notable drop in PSNR and SSIM values clearly reveals that the noise disrupts the visual similarity of the watermark. Similarly, low NC values indicate that the similarity between the extracted watermark and the original one is reduced. In the JPEG compression attack, the effects on the watermark were also prominent. The decrease in SSIM and NC values suggests that structural losses occurred after compression. Particularly in the W2 watermark, quality loss became more evident. The sharpening attack proved to be one of the most destructive. Significant drops were observed in all quality metrics as a result of this attack. While PSNR values decreased considerably, SSIM and NC values also suffered substantial reductions. This demonstrates that sharpening severely degrades both the structural integrity and perceptibility of the watermark.

Overall, it was observed that the proposed method demonstrates a certain level of robustness against attacks with a low scaling factor, but decreases in quality metrics were inevitable. Increasing the scaling factor could enhance watermark robustness; however, it was not preferred in this study as it would cause distortion in medical images. Since the primary objective of the study is to preserve the integrity of medical images, a scaling factor of 0.01 offers the ideal balance. This factor ensures acceptable watermark extraction success with minimal distortion. The hybrid DCT-SVD-based invisible watermarking techniques developed in this study offer significant potential, particularly for protecting information privacy in medical images. However, to further enhance the performance of these methods, certain improvements and advanced applications are needed.

In particular, in the Second Method, the block selection strategy has a direct impact on performance. Therefore, smarter block selection algorithms can be developed to improve the results. In this context, block selection techniques guided by mathematical modeling or based on statistical features may be applied.

Furthermore, the integration of artificial intelligence-based optimization algorithms can enable the automation of watermark placement. Techniques such as genetic algorithms, particle swarm optimization (PSO), or artificial neural networks can be used to optimize the placement region and size of the watermark, resulting in more efficient outcomes in terms of both robustness and confidentiality. Indeed, in a study conducted by [22] using the Moth-Flame Optimization algorithm, the effectiveness of optimization-based approaches in the image segmentation process was demonstrated; this may serve as a guiding framework for the integration of similar optimization techniques into invisible watermarking processes.

For future studies, it is recommended to explore not only DCT-SVD but also methods involving different transform domains. In particular, alternative frequency-based hybrid approaches such as SVD-based DWT (DWT-SVD) or SVD-based DFT (DFT-SVD) could lead to the development of more robust and attack-resistant watermarking techniques. Such techniques can offer higher protection in terms of both security and data integrity in medical imaging.

Data Availability Statement

Data will be made available on request.

Funding

This work was supported without any funding.

Conflicts of Interest

The authors declare no conflicts of interest.

AI Use Statement

The authors declare that no generative AI was used in the preparation of this manuscript.

Ethical Approval and Consent to Participate

Not applicable.

References

[1] Solachidis, V., & Pitas, L. (2001). Circularly symmetric watermark embedding in 2-D DFT domain. *IEEE transactions on image processing, 10*(11), 1741-1753. [CrossRef]

[2] Mohammed, A. A., Jebur, B. A., & Younus, K. M. (2021, May). Hybrid DCT-SVD based digital watermarking scheme with chaotic encryption for medical images. In *IOP Conference Series: Materials Science and Engineering* (Vol. 1152, No. 1, p. 012025). IOP Publishing. [CrossRef]

[3] Zain, J. M., & Clarke, M. (2011). Reversible region of non-interest (RONI) watermarking for authentication of DICOM images. *arXiv preprint arXiv:1101.1603*.

[4] Karakış, R., & Gurkahraman, K. (2021). TIBBİ GÖRÜNTÜLERİN GÜVENLİĞİ İÇİN İLGİ OLMAYAN BÖLGELERDE KENAR TABANLI DAMGALAMA. *Adıyaman Üniversitesi Mühendislik Bilimleri Dergisi*, *8*(14), 154–168.

[5] Mamuti, M., & Kazan, S. (2019). A novel digital image watermarking scheme for medical image. *Int J Comput Sci Mob Comput*, *8*(4), 198-203.

[6] Alghoniemy, M., & Tewfik, A. H. (2004). Geometric invariance in image watermarking. *IEEE Transactions on Image Processing*, *13*(2), 145-153. [CrossRef]

[7] Aslantas, V. (2009). SVD and DWT-SVD domain robust watermarking using differential evolution algorithm. In *Advances in Electrical Engineering and Computational Science* (pp. 147-159). Dordrecht: Springer Netherlands. [CrossRef]

[8] Aslantas, V., Dogan, A. L., & Ozturk, S. (2008, June). DWT-SVD based image watermarking using particle swarm optimizer. In *2008 IEEE international conference on multimedia and expo* (pp. 241-244). IEEE. [CrossRef]

[9] Aslantas, V., & Oz, A. Diferansiyel Gelişim Algoritması İle Tekil Değer Ayrışımına Dayalı Resim Damgalama. *ISC Turkey*, 3-5.

[10] Furat, M., & Oral, M. (2007). Digital image watermarking based on a relation between spatial and frequency domains. In *5th International Conference on Electrical and Electronics Engineering* (*ELECO 2007*).

[11] Dogan, S., Tuncer, T., Avci, E., & Gulten, A. (2011). A robust color image watermarking with Singular Value Decomposition method. *Advances in Engineering Software*, *42*(6), 336–346. [CrossRef]

[12] Ustubioglu, A., & Ulutas, G. (2017). A new medical image watermarking technique with finer tamper localization. *Journal of digital imaging*, *30*(6), 665-680. [CrossRef]

[13] Priyanka, & Maheshkar, S. (2017). Region-based hybrid medical image watermarking for secure telemedicine applications. *Multimedia Tools and Applications*, *76*(3), 3617-3647. [CrossRef]

[14] Yıldız, S., Üstünsoy, F., & Sayan, H. H. (2023). Digital image watermarking with hybrid structure of DWT, DCT, SVD techniques and the optimization with BFO algorithm. *Politeknik Dergisi*, *27*(3), 857-871. [CrossRef]

[15] Yang, H. Y., Wang, X. Y., Niu, P. P., & Wang, A. L. (2015). Robust color image watermarking using geometric invariant quaternion polar harmonic transform. *ACM Transactions on Multimedia Computing, Communications, and Applications* (*TOMM*), *11*(3), 1-26. [CrossRef]

[16] Balcı, D., Karakış, R., & Güler, İ. (2020). Tıbbi DICOM Veri Güvenliğinde Hibrit Yöntemlerin Kullanılması. *Düzce Üniversitesi Bilim ve Teknoloji Dergisi*, *8*(2), 1295–1306. [CrossRef]

[17] OKEDIRAN, O. O. (2019). A security scheme for patient information Privacy in digital medical imaging. *University of Pitesti Scientific Bulletin Series: Electronics and Computer Science*, *19*(2), 13-24.

[18] Karakış, R., Güllü, M. K., Çavusoğlu, Ü., Kaçar, S., & Pehlivan, İ. (2015). A novel fuzzy logic-based image steganography method to ensure medical data security. *Computers in biology and medicine*, *67*, 172–183. [CrossRef]

[19] Hore, A., & Ziou, D. (2010, August). Image quality metrics: PSNR vs. SSIM. In *2010 20th international conference on pattern recognition* (pp. 2366-2369). IEEE. [CrossRef]

[20] Kurban, R., & Bozpolat, H. (2022). Ayrık Kosinüs Dönüşümü DC Bileşenleri Ve Çoklu-Adaptif Ölçekleme Faktörleri Kullanılarak Dayanıklı Görüntü Damgalama. *Eskişehir Osmangazi Üniversitesi Mühendislik ve Mimarlık Fakültesi Dergisi*, *30*(2), 190–200. [CrossRef]

[21] Gomez-Coronel, S. L., Mascorro-Cano, J. A., Cedillo-Hernandez, M., Cedillo-Hernandez, A., Nakano-Miyatake, M., & Perez-Meana, H. (2023). A robust and secure watermarking approach based on hermite transform and SVD-DCT. *Applied Sciences*, *13*(14), 8430. [CrossRef]

[22] Karakoyun, M. (2023). The comparison of the effects of thresholding methods on segmentation using the moth flame optimization algorithm. *Journal of Engineering Sciences*, *26*(2), 517–531.

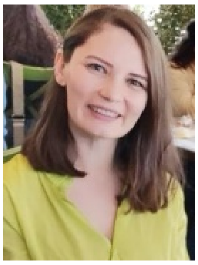

Emine Aksu received the B.Sc. degree in Computer Engineering from the Faculty of Engineering and Architecture, Selçuk University, in 2014. She obtained the M.Sc. degree in Industrial Engineering from the Graduate School of Natural and Applied Sciences, Necmettin Erbakan University, in 2024. (Email: emineuzunkaya1@gmail.com)

Murat Karakoyun received the Ph.D. degree from the Department of Computer Engineering of Konya Technical University. He is working as a Assoc. Prof. at Computer Engineering Department of Necmettin Erbakan University. His working topics are artificial intelligence, image processing, data mining, machine learning, optimization etc. (Email: mkarakoyun@erbakan.edu.tr)